中國機械工程學刊第四十五卷第三期第 201~208 頁(民國一百一十三年)
Journal of the Chinese Society of Mechanical Engineers, Vol.45, No.3, pp201~208 (2024)

Response and Failure of Elliptical Tubes With Different Long/Short Axis Ratios Under Cyclic Bending

Min-Cheng Yu* and Wen-Fung Pan**

Keywords: SUS304 stainless steel elliptical tubes, long/short axis ratios, moment-curvature relationships, short axis variation-curvature relationships, cyclic bending, buckling failure.

ABSTRACT

This paper investigates the response and failure of SUS304 stainless steel elliptical tubes with four different long/short axis ratios (1.5, 2.0, 2.5, and 3.0) under cyclic bending. The wall thickness is 0.7 mm for all elliptical tubes, and cyclic bending loads are applied until buckling failure occurs. The experimental moment-curvature relationships exhibit cyclic hardening and form stable loops for all long/short axis ratios. An increase in the long/short axis ratio results in a slight decrease in the peak bending moment. The experimental relationships between short axis variation and curvature (where short axis variation represents the change in the length of the short axis divided by the original length of the short axis) demonstrate symmetry, serrations, and a growth pattern as cycles progress, regardless of the long/short axis ratio. Interestingly, when long/short axis ratios are equal to 2.0, 2.5, and 3.0, the relationships even exhibit butterfly-like trends. Moreover, a larger long/short axis ratio corresponds to a greater short axis variation. Regarding the curvature-number of cycles required to initiate buckling relationships, it can be observed that the four long/short axis ratios correspond to four straight lines when plotted on double logarithmic coordinates. Lastly, this study proposes theoretical equations to describe the aforementioned relationships. The theoretical analysis is compared with experimental data, revealing a close alignment between the two approaches. This indicates that the theory can reasonably describe the experimental results.

Paper Received August, 2023. Revised December, 2023. Accepted March, 2024. Author for Correspondence: Wen-Fung Pan.

* *Graduate Student, Department of Engineering Science, National Cheng Kung University, Tainan, Taiwan 70101, ROC.*

** *Professor, Department of Engineering Science, National Cheng Kung University, Tainan, Taiwan 70101, ROC.*

INTRODUCTION

Traditional circular tubes are commonly employed as pipes or support structures. However, they exhibit limitations in terms of load-bearing capacity, wear resistance, and shock absorption. In contrast, elliptical tubes offer several advantages, including enhanced fluid dynamics, superior load-bearing capacity, heightened wear resistance, and increased shock absorption. By capitalizing on these benefits and combining them with the excellent properties of SUS304 stainless steel, such as corrosion resistance, high ductility, ease of processing, and strong tensile strength. SUS304 stainless steel elliptical tubes (as depicted in Fig. 1) find extensive applications across various domains.

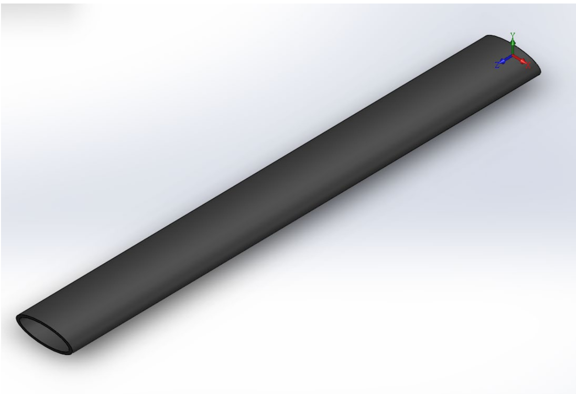

Fig. 1. Schematic diagram of an elliptical tube.

Nonetheless, elliptical tubes often encounter the challenge of enduring cyclic bending loads. These loads induce a gradual reduction in bending rigidity as the bending moment increases or as the number of cycles rises. This phenomenon is referred to as the degradation phenomenon, with the short axis variation serving as an apt descriptor of this behavior. Eventually, buckling failure transpires when the short axis variation surpasses a critical threshold.

So far, significant progress has been achieved in the study of bending behaviors exhibited by smooth circular tubes. In 1987, Kyriakides and Shaw (1987) developed a mechanical apparatus capable of conducting monotonic or cyclic bending tests on circular tubes with or without external pressure. The materials investigated encompassed 1020 steel, 1018 steel, 304 stainless steel, 6061-T6 aluminum alloy, and NiTi circular smooth tubes (Kyriakides and Shaw, 1987; Corona and Kyriakides, 1991; Corona and Kyriakides, 2000; Corona et al., 2006; Limam et al., 2010; Limam et al., 2012; Bechle and Kyriakides, 2014; Jiang et al., 2017; Kazinakis et al., 2019). Other researchers have similarly reported relevant findings. For instance, Yuan and Mirmiran (2001) examined the buckling behavior of fiber-reinforced concrete-filled plastic pipes, Elchalakani et al. (2006) ascertained the slenderness limit of cold-formed CHS (circular hollow sections) featuring fully ductile profiles by conducting cyclic bending tests at varying amplitudes. Houliara and Karamanos (2006) explored the in-phase bending buckling response of tubes subject to external pressure, Yazdani and Nayebi (2013) investigated the damage sustained by pipes undergoing periodic bending while under steady internal pressure, Elchalakani et al. (2016) employed strains observed in bending tests to establish novel ductile slenderness limits for the plastic design of concrete-filled-tube structures, Shamass et al. (2017) delved into the instability of circular tubes following non-proportional paths, Li and Wang (2018) examined the instability of a single-layer cable-reinforced reticulated shell when subjected to seismic forces, and Chegeni et al. (2019) explored the impact of corrosion depth and shape on the performance of curved pipes under specific internal pressure conditions.

Pan et al. (1998) developed a device in 1988, which enables the measurement of curvature and ovalization of circular tubes during bending. Their work involved a range of bending experiments on smooth circular tubes, including cyclic bending experiments (Lee et al., 2001), viscoplastic cyclic bending experiments (Pan and Her, 1998), pure bending creep experiments (Lee and Pan, 2002), cyclic bending experiments with varying mean curvatures (Pan and Lee, 2002), and cyclic bending experiments with varying mean moments (Chang et al., 2008).

Starting from 2010, Pan et al. shifted their focus towards investigating the behavior of notched circular tubes under bending loads. For instance, they conducted cyclic bending tests on circular tubes featuring circumferential sharp notches (Lee et al., 2010; Lee et al., 2013; Chung et al., 2016), as well as cyclic bending tests on circular tubes incorporating localized sharp dents (Lee et al., 2016). Furthermore, Lee and colleagues conducted a series of studies on the response of different types of tubes (sharp-notched circular tubes (Lee et al., 2018), and round-hole tubes (Lee et al., 2019; Lee et al., 2021)) under cyclic bending.

Given the absence of pertinent research concerning the behavior of elliptical tubes under bending loads, this paper aims to investigate the response and failure of SUS304 stainless steel elliptical tubes when under cyclic bending loads. The study encompasses four distinct long/short axis ratios: 1.5, 2.0, 2.5, and 3.0. To achieve this, cyclic bending tests were conducted utilizing appropriate experimental apparatus. Simultaneously, various parameters including the bending moment, curvature, short axis variation, and the number of cycles required to initiate buckling were meticulously measured and analyzed.

EXPERIMENTS

Bending Devices

In this study, a four-point bending machine was utilized to conduct cyclic bending tests on SUS304 stainless steel elliptical tubes, as depicted in Fig. 2. The setup comprises two rotating sprockets positioned on two supporting beams. A robust chain runs around these sprockets, which are supported by heavy-duty beams. This configuration allows for test specimens with a maximum length of 1 meter. To facilitate the testing, each tube is outfitted with solid rod extensions, as illustrated in Fig. 3. Throughout the bending process, the interaction between the tube and the roller permits free axial movement. The load applied to the test specimen is generated by means of two concentrated loads originating from a pair of rollers. Upon retraction of the upper or lower cylinder, the sprocket initiates rotation, facilitating pure bending of the test specimen. To achieve reverse bending, the hydraulic circuit's flow direction is reversed.

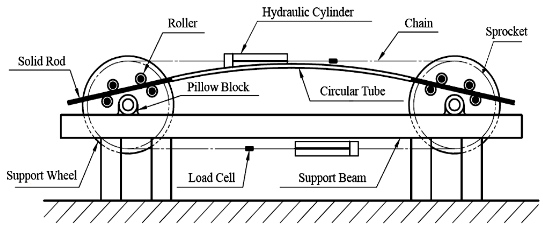

Fig. 2. Schematic diagram of the tube-bending machine.

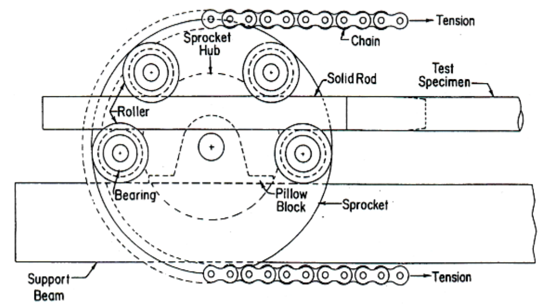

Fig. 3. Enlarged schematic diagram of the sprocket.

Nonetheless, the spatial confines of the rollers solely accommodate the insertion of solid rods with circular cross-sections, as depicted in Fig. 3. Inserting a solid rod with a circular cross-section into the elliptical tube proves unfeasible. To address this challenge, this study undertakes necessary adaptations to the solid rod design. As illustrated in Fig. 4, a new solid rod configuration is devised for use with the tube-bending machine. The disassembled configuration of the elliptical tube and the newly designed solid rod is outlined in Fig. 5, while Fig. 6 presents an exploded view of the newly designed solid rod. These figures show that the newly devised solid rod combines an elliptical cross-section on one side and a circular cross-section on the other. The fusion of these components is achieved through welding on both contact surfaces, resulting in the creation of the novel solid rod. Given that this investigation involves four distinct long/short axis ratios, the elliptical cross-section solid rods on one side must be of varying sizes – four sizes to be precise. Conversely, the circular cross-section solid rods on the other side maintain a consistent size, as shown in Fig. 7.

Curvature-Ovalization Measurement Apparatus (COMA)

The COMA devised by Pan et al. (1998), shown in Fig. 8, serves as a tool for gauging tube curvature and the cross-sectional ovalization of tubes. Ovalization is defined as the alteration of the outer diameter divided by the original outer diameter. This lightweight instrument is conveniently situated in proximity to the mid-span of the tube. Leveraging the fixed spacing between the two side-inclinometers and the angular shifts identified by these inclinometers, tube curvature can be easily computed. Furthermore, the COMA incorporates a magnetic detector positioned at its center to assess alterations in the outer diameter, enabling the determination of tube's ovalization. In this particular study, the COMA was employed to track variations in the short axis of the elliptical tube, thereby facilitating the acquisition of short axis changes. A detailed exposition of the COMA can be found in the work by Pan et al. (1998).

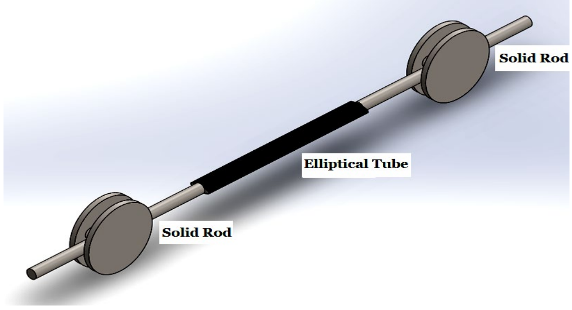

Fig. 4. Schematic diagram of the newly designed solid rod erected on the tube-bending machine.

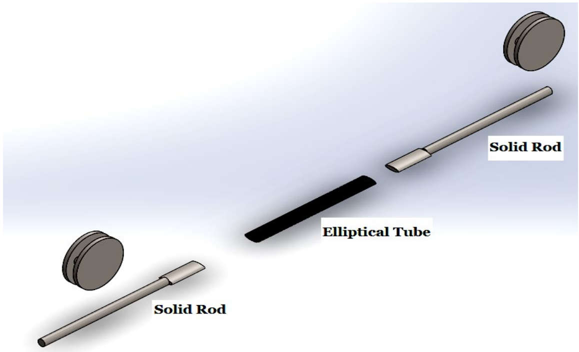

Fig. 5. Disassembled diagram of the elliptical tube and the newly designed solid rod.

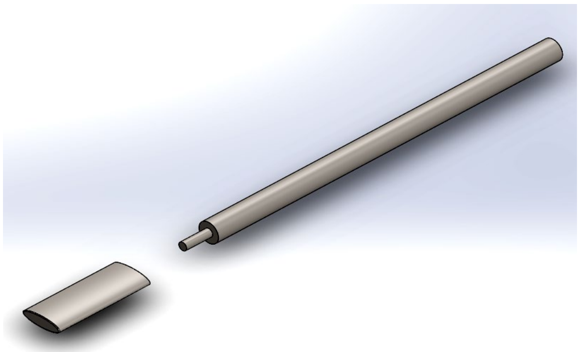

Fig. 6. Schematic diagram of the exploded view of the newly designed solid rod.

Fig. 7. Picture of four solid rods.

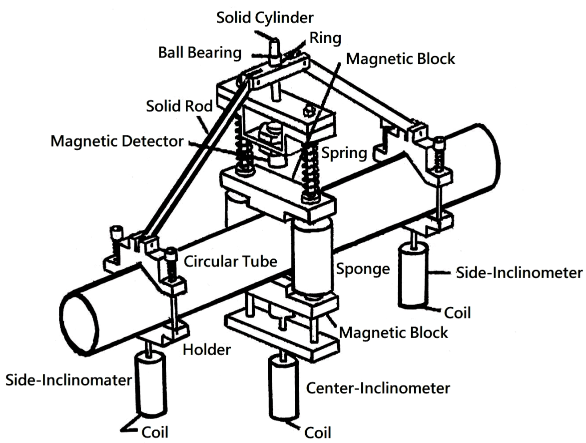

Fig. 8. Schematic diagram of the COMA.

Elliptical Tubes

The experiment utilized the SUS304 stainless steel elliptical tubes, and Tables 1 and 2 respectively show the chemical composition and mechanical properties of the SUS304 stainless steel. The length of the elliptical tubes is 500 mm, with a thickness of 0.7 mm. Fig. 9 shows the schematic diagram of the long axis and short axis of the cross-section of an elliptical tube. In this study, four different long/short axis ratios (ℓ_{long}/ℓ_{short} ratios), 1.5 (30mm/20mm), 2.0 (40mm/20mm), 2.5 (50mm/20mm), and 3.0 (60mm/20mm) were considered as shown in Fig. 10.

Table 1. Chemical composition of the SUS304 stainless steel (weight %)

Element	Fe	Cr	Ni	Mn	Si	C	P
Proportion (%)	72.36	18.01	8.01	1.01	0.51	0.08	0.011

Table 2. Mechanical properties of the SUS304 stainless steel.

Density	7930 Kg/m^3
Young's Modulus	195 GPa
Poisson's Ratio	0.33
Yield Strength	296 MPa
Ultimate Strength	626 MPa

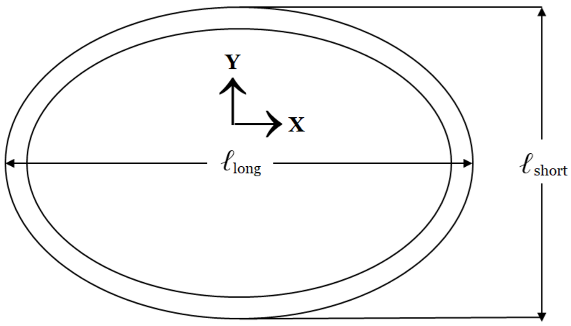

Fig. 9. Schematic diagram illustrating the long axis and short axis of the cross-section of an elliptical tube.

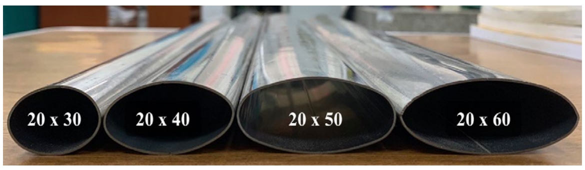

Fig. 10. Picture of SUS304 stainless steel elliptical tubes with four different ℓ_{long}/ℓ_{short} ratios.

Test Procedures

The experiment entailed a curvature-controlled cyclic bending test, characterized by a curvature rate of 0.05 $m^{-1}s^{-1}$. In this investigation, the direction of the bending moment coincided with the long axis direction, specifically the x-direction, as shown in both the 3D Fig. 1 and 2D Fig. 9. This bending load condition is common to most elliptical tubes. The controlled- curvature ranges spanned from -0.5 m^{-1} to +0.5 m^{-1}, and extended further to -0.8 m^{-1} to +0.8 m^{-1}. The bending moment (M) was ascertained through load cells incorporated into the bending machine, as depicted in Fig. 2. The curvature (κ) and short axis variation ($\Delta\ell/\ell_{short}$, where $\Delta\ell$ is the change in ℓ_{short}) were measured by the apparatus in Fig. 8. Simultaneously, the number of cycles required to initiate buckling (N_b) was recorded.

RESULTS AND DISCUSSION

M-κ Relationships

Figs. 11(a)-11(d) respectively present the experimental *M-κ* relationships of SUS304 stainless steel elliptical tubes with ℓ_{long}/ℓ_{short} ratios = 1.5, 2.0, 2.5, and 3.0 under cyclic bending. The κ was controlled within the range of +0.5 m^{-1} to -0.5 m^{-1}. During the initial loading stage, the elliptical tube is within the elastic range, resulting in a linear growth in the *M-κ* relationship. As κ increases, the elliptical tube starts to deform plastically, leading to a gradual flattening of the *M-κ* relationship and causing permanent deformation. The experimental results also show that all *M-κ* curves exhibit cyclic hardening and become stable after a few cycles. Additionally, under the same κ, as the ℓ_{long}/ℓ_{short} ratio increases, the peak value of M gradually decreases. For instance, when ℓ_{long}/ℓ_{short} ratio is 1.5, the peak M value is ±108 N-m; while for ℓ_{long}/ℓ_{short} ratio of 3.0, the peak M value reduces to ±88 N-m. Notably, different κ all exhibit similar phenomena. Therefore, this study only presents the *M-κ* relationship for κ = ±0.5 m^{-1} and ℓ_{long}/ℓ_{short} ratios of 1.5, 2.0, 2.5, and 3.0.

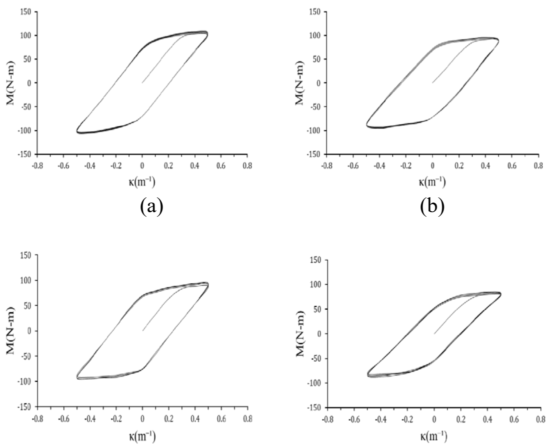

Fig. 11. Experimental *M-κ* relationships of SUS304 stainless steel elliptical tubes with ℓ_{long}/ℓ_{short} ratio = (a)1.5, (b)2.0, (c)2.5, and (d)3.0 under cyclic bending.

$\Delta\ell/\ell_{short}$-*κ* Relationships

Figs. 12(a)-12(d) showcase the experimental $\Delta\ell/\ell_{short}$-κ relationships of SUS304 stainless steel elliptical tubes with ℓ_{long}/ℓ_{short} ratios = 1.5, 2.0, 2.5, and 3.0 under cyclic bending. The κ values were similarly confined within the range of +0.5 m^{-1} to -0.5 m^{-1}. Evidently, when considering an ℓ_{long}/ℓ_{short}

ratio of 1.5, the $\Delta\ell/\ell_{short}$-κ relationship follows a pattern marked by symmetry, ratcheting, and incremental growth as the cycling progresses. Due to the ℓ_{long}/ℓ_{short} ratio approaches a circular cross-section, the $\Delta\ell/\ell_{short}$-κ trend resembles that of a circular tube. As the ℓ_{long}/ℓ_{short} ratio increases, signifying a stretching of the long axis, the elliptical tube's cross-section tends toward an oblate configuration. Consequently, under the same κ value, a higher ℓ_{long}/ℓ_{short} ratio corresponds to a more pronounced $\Delta\ell/\ell_{short}$. Notably, for ℓ_{long}/ℓ_{short} ratios $\geq$ 2.0, the $\Delta\ell/\ell_{short}$-κ relationship showcases a symmetrical, ratcheting, incremental growth, and even butterfly-like pattern.

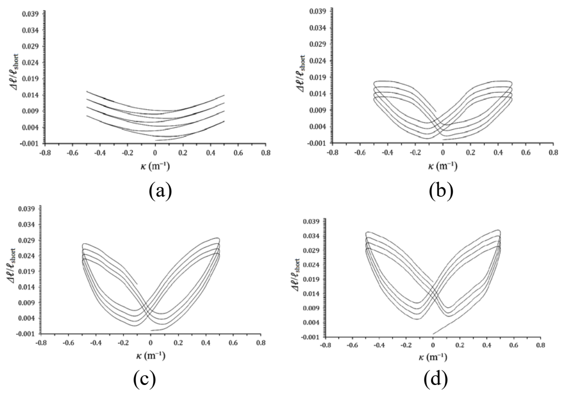

Fig. 12. Experimental $\Delta\ell/\ell_{short}$-κ relationships of SUS304 stainless steel elliptical tubes with ℓ_{long}/ℓ_{short} ratio = (a)1.5, (b)2.0, (c)2.5, and (d)3.0 under cyclic bending.

κ-N_b Relationships

Fig. 13 presents the experimental κ-N_b relationships of SUS304 stainless steel elliptical tubes with four different ℓ_{long}/ℓ_{short} ratios under cyclic bending. Notably, as observed from the figure, when maintaining a constant ℓ_{long}/ℓ_{short} ratio, N_b diminishes with an increase in κ. Similarly, for a consistent κ, N_b experiences a decline as the ℓ_{long}/ℓ_{short} ratio increases. In Fig. 14, the identical data showcased in Fig. 13 are depicted on a double logarithmic scale. The straight lines featured on the plot are outcomes of the least squares method. Upon examining the plot, it becomes evident that the four distinct ℓ_{long}/ℓ_{short} ratios correspond to four straight lines.

In 1987, Kyriakides and Shaw (1987) proposed the κ/κ_o-N_b relationship for smooth circular tubes under cyclic bending loads to be:

$$\kappa/\kappa_o = C(N_b)^{-\alpha} \tag{1}$$

or

$$\log \kappa/\kappa_o = \log C - \alpha \log N_b, \tag{2}$$

where κ_o is utilized to represent the dimensionless parameter κ, which is defined as the tube thickness divided by the square of the outer diameter, while C and α are material parameters. C signifies the value of κ/κ_o when N_b equals 1, and α denotes the slope of the straight line in the κ/κ_o-N_b relationship on double logarithmic coordinates. Since the current experiment employs elliptical tubes, determining κ_o becomes infeasible. Consequently, Eq. (1) is expressed as follows:

$$\kappa = C(N_b)^{-\alpha} \tag{3}$$

or

$$\log \kappa = \log C - \alpha \log N_b, \tag{4}$$

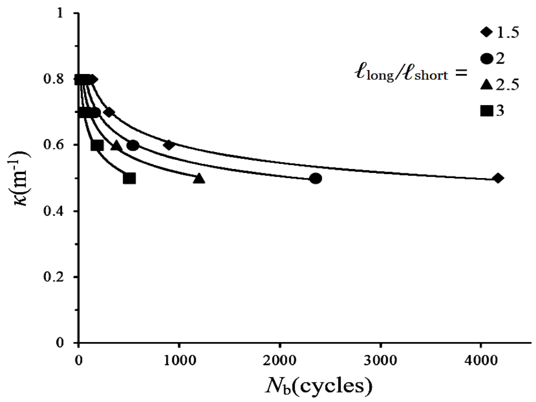

Fig. 13. Experimental κ-N_b relationships of SUS304 stainless steel elliptical tubes with four different ℓ_{long}/ℓ_{short} ratios under cyclic bending.

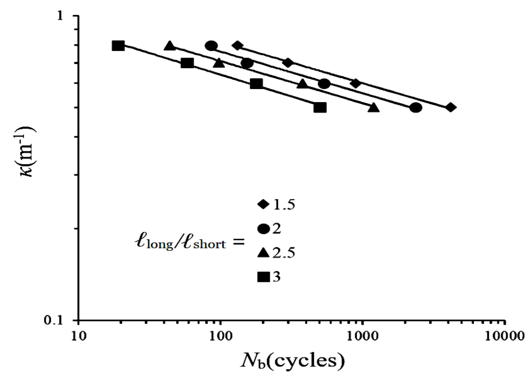

Fig. 14. Experimental κ-N_b relationships of SUS304 stainless steel elliptical tubes with four different ℓ_{long}/ℓ_{short} ratios under cyclic bending on double logarithmic coordinates.

Based on the experimental data, the relationships between log$C$ and ℓ_{long}/ℓ_{short} ratios, as well as between α and ℓ_{long}/ℓ_{short} ratios were fitted and depicts in Fig. 15 and Fig. 16, respectively. The straight lines in the plots were obtained through the least squares regression fitting method. The linear trends observed in these relationships enable the formulation of the following expressions:

$$\log C = c_1(\ell_{long}/\ell_{short}) + c_2 \tag{5}$$

and

$$\alpha = a_1(\ell_{long}/\ell_{short}) + a_2 \tag{6}$$

where c_1, c_2, a_1, and a_2 are material parameters, which can be obtained from the fitting of the relationships between $\log C$ and ℓ_{long}/ℓ_{short} ratios, and α andℓ_{long}/ℓ_{short} ratios, as shown in Fig. 15 and Fig. 16. The specific material parameters are calculated to be c_1 = -0.0613, c_2 = 0.2777, a_1 = 0.005, and a_2 = 0.127. Conclusively, Eqs. (3), (5), and (6) were employed to characterize the κ-N_b relationships of SUS304 stainless steel elliptical tubes with different ℓ_{long}/ℓ_{short} ratios under cyclic bending. The outcomes of theoretical analysis are depicted as dashed lines in Fig. 17. Through comparison with the experimental results, it is evident that that the formulations introduced in this study adequately and reasonably describe the experimental finding.

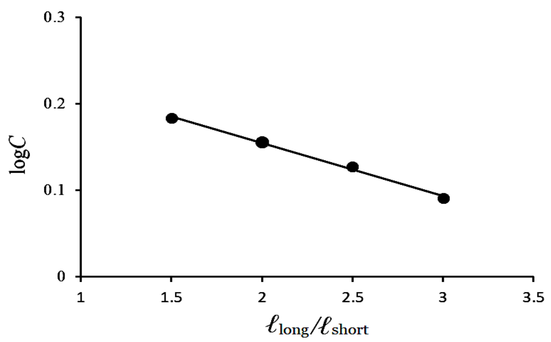

Fig. 15. Relationship between $\log C$ and ℓ_{long}/ℓ_{short} ratios.

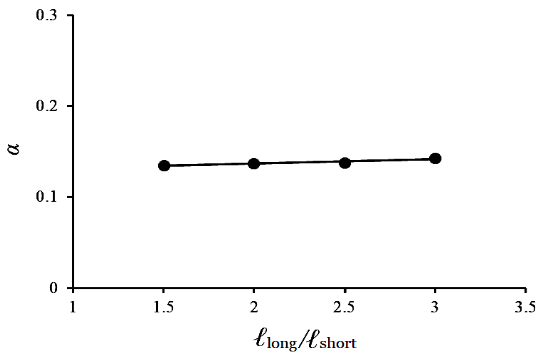

Fig. 16. Relationship between α and ℓ_{long}/ℓ_{short} ratios.

CONCLUSIONS

This study delves into the behavior and failure mechanisms of SUS304 stainless steel elliptical tubes with four different ℓ_{long}/ℓ_{short} ratios of 1.5, 2.0, 2.5, and 3.0 under cyclic bending. Based on both experimental findings and theoretical analyses, several key conclusions can be drawn from this research:

(1) The M-κ relationships for different ℓ_{long}/ℓ_{short} ratios reveal a slight cyclic hardening tendency, ultimately stabilizing into elastic-plastic loops after several cycles. Notably, with consistent κ loading, increasing the ℓ_{long}/ℓ_{short} ratio leads to a gradual reduction in the peak M value.

(2) The experimental $\Delta\ell/\ell_{short}$-κ relationships exhibit distinct trends based on ℓ_{long}/ℓ_{short} ratio. When the ℓ_{long}/ℓ_{short} ratio is 1.5, the $\Delta\ell/\ell_{short}$-κ curves show symmetry, serrations, and a growth pattern as cycles progress. When the ℓ_{long}/ℓ_{short} ratio surpasses 2.0, the $\Delta\ell/\ell_{short}$-κ relationship showcases a symmetrical, serrated, growing, and even butterfly-like pattern. In addition, under the same κ loading condition, a larger ℓ_{long}/ℓ_{short} ratio results in a larger $\Delta\ell/\ell_{short}$.

(3) Analysis of the experimental κ-N_b relationships reveals that, while holding ℓ_{long}/ℓ_{short} ratio constant, N_b decreases with increasing κ. Similarly, at a fixed κ, N_b declines with elevated ℓ_{long}/ℓ_{short} ratio. To describe the κ-N_b relationships, Eq. (3) was introduced. Capitalizing on experimental data, Eqs. (5) and (6) were derived. Ultimately, Eqs. (3), (5), and (6) were employed to describe the κ-N_b relationships for SUS304 stainless steel elliptical tubes with different ℓ_{long}/ℓ_{short} ratios under cyclic bending. The theoretical calculations closely matched the experimental data, as illustrated in Fig. 17.

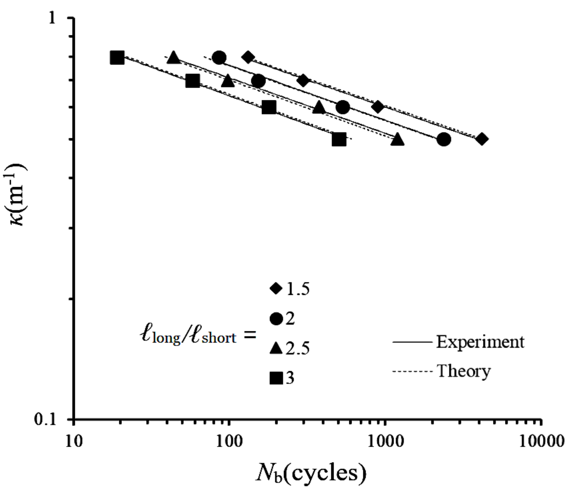

Fig. 17. Experimental and theoretical κ-N_b relationships of SUS304 stainless steel elliptical tubes with different ℓ_{long}/ℓ_{short} ratios under cyclic bending on double logarithmic coordinates.

ACKNOWLEDGMENT

The research was conducted with the generous support of the National Science and Technology Council, through grant NSTC 112–2221–E–006–174. We extend our heartfelt gratitude for their invaluable assistance.

REFERENCES

Bechle, N.J. and Kyriakides, S., "Localization of NiTi Tubes under Bending," *Int. J. Solids Struct.*, Vol. 51, No. 5, pp. 967-980 (2014).

Chang, K.H., Pan, W.F. and Lee, K.L., "Mean Moment Effect of Thin-Walled Tubes under Cyclic Bending," *Struct. Eng. Mech.*, Vol. 28, No. 5, pp. 505-535 (2008).

Chegeni, B., Jayasuriya, S. and Das, S., "Effect of Corrosion on Thin-Walled Pipes under Combined Internal Pressure and Bending," *Thin-Walled Struct.*, Vol. 143, 106218 [8 pages] (2019).

Chung, C.C., Lee, K.L. and Pan, W.F., "Collapse of Sharp-notched 6061-T6 Aluminum Alloy Tubes under Cyclic Bending," *Int. J. Struct. Stab. Dyn.*, Vol. 26, No. 7, 1550035 [24 pages] (2016).

Corona, E. and Kyriakides, S., "An Experimental Investigation of the Degradation and Buckling of Circular Tubes under Cyclic Bending and External Pressure," *Thin-Walled Struct.*, Vol. 12, No. 3, pp. 229-263 (1991).

Corona, E. and Kyriakides, S., "Asymmetric Collapse Modes of Pipes under Combined Bending and Pressure," *Int. J. Solids Struct.*, Vol. 24, No. 5, pp. 505-535 (2000).

Corona, E., Lee, L.H. and Kyriakides, S., "Yield Anisotropic Effects on Buckling of Circular Tubes under Bending," *Int. J. Solids Struct.*, Vol. 43, No. 22, pp. 7099-7118 (2006).

Elchalakani, M., Karrech¸ A., Hassanein, M.F. and Yang, B., "Plastic and Yield Slenderness Limits for Circular Concrete Filled Tubes Subjected to Static Pure Bending," *Thin-Walled Struct.*, Vol. 109, pp. 50-64 (2016).

Elchalakani, M., Zhao, X.L. and Grzebieta, R.H., "Variable Amplitude Cyclic Pure Bending Tests to Determine Fully Ductile Section Slenderness Limits for Cold-Formed CHS," *Eng. Struct.*, Vol. 28, No. 9, pp. 1223-1235 (2006).

Houliara, S. and Karamanos, S.A., "Buckling and Post-Buckling of Long Pressurized Elastic Thin-Walled Tubes under In-Plane Bending," *Int. J. Nonlinear Mech.*, Vol. 41, No. 4, pp. 491-511 (2006).

Jiang, D., Kyriakides, S., Bechle, N.J. and Landis, C.M., "Bending of Pseudoelastic NiTi Tubes," *Int. J. Solids Struct.*, Vol. 124, pp. 192-214 (2017).

Kazinakis, K., Kyriakides, S., Jiang, D., Bechle, N.J. and Landis, C.M., "Buckling and Collapse of Pseudoelastic NiTi Tubes under Bending," *Int. J. Solids Struct.*, Vol. 221, pp. 2-7 (2021).

Kyriakides, S. and Shaw, P.K., "Inelastic Buckling of Tubes under Cyclic Loads," *ASME J. Press. Ves. Tech.*, Vol. 109, No. 2, pp. 169-178 (1987).

Lee, K.L., Chang, K.H. and Pan, W.F., "Failure Life Estimation of Sharp-Notched Circular Tubes with Different Notch Depths under Cyclic Bending," *Struct. Eng. Mech.*, Vol. 60, No. 3, pp. 387-404 (2016).

Lee, K.L., Chang, K.H. and Pan, W.F., "Effects of Notch Depth and Direction on Stability of Local Sharp-Notched Circular Tubes Subjected to Cyclic Bending," *Int. J. Struct. Stab. Dyn.*, Vol. 18, No. 7, 1850099 [23 pages] (2018).

Lee, K.L., Hsu, C.M. and Pan, W.F., "Viscoplastic Collapse of Sharp-Notched Circular Tubes under Cyclic Bending," *Acta Mech. Solida Sinica*, Vol. 26, No. 6, pp. 629-641 (2013).

Lee, K.L., Hung, C.Y. and Pan, W.F., "Variation of Ovalization for Sharp-Notched Circular Tubes under Cyclic Bending," *J. Mech.*, Vol. 26, No. 3, pp. 403-411 (2010).

Lee, K.L. and Pan, W.F., "Pure Bending Creep of SUS304 Stainless Steel Tubes," *Steel Comp. Struct.*, Vol. 2, No. 6, pp. 461-474 (2002).

Lee, K.L., Pan, W.F. and Kuo, J.N., "The Influence of the Diameter-to-Thickness Ratio on the Stability of Circular Tubes under Cyclic Bending," *Int. J. Solids Struct.*, Vol. 38, No. 14, pp. 2401-2413 (2001).

Lee, K.L., Tsai, Y.C. and Pan, W.F., "Mean Curvature Effect on the Response and Failure of Round-Hole Tubes Submitted to Cyclic Bending," *Adv. Mech. Eng.*, Vol. 13, No. 11, pp. 1-14 (2021).

Lee, K.L., Weng, M.L. and Pan, W.F., "On the Failure of Round-Hole Tubes under Cyclic Bending," *J. Chi. Soc. Mech. Eng.*, Vol. 40, No. 6, pp. 663-673 (2019).

Li, P. and Wang, L., "Nonlinear Stability Behavior of Cable-Stiffened Single-Layer Latticed Shells under Earthquakes," *Int. J. Struct. Stab. Dyn.*, Vol. 18, No. 10, 1850117 [24 pages] (2018).

Limam, A., Lee, L.H. and Kyriakides, S., "On the Collapse of Dented Tubes under Combined Bending and Internal Pressure," *Int. J. Solids Struct.*, Vol. 55, No. 1, pp. 1-12 (2012).

Limam, A., Lee, L.H., Corona, E. and Kyriakides, S., "Inelastic Wrinkling and Collapse of Tubes under Combined Bending and Internal Pressure," *Int. J. Mech. Sci.*, Vol. 52, No. 5, pp. 37-47 (2010).

Pan, W.F. and Her, Y.S., "Viscoplastic Collapse of Thin-Walled Tubes under Cyclic Bending," *ASME J. Eng. Mat. Tech.*, Vol. 120, No. 4, pp. 287-290 (1998).

Pan, W.F. and Lee, K.L., "The Effect of Mean Curvature on the Response and Collapse of Thin-Walled Tubes under Cyclic Bending," *JSME Int. J.*, *Ser. A*, Vol. 28, No. 2, pp. 495-514 (2002).

Pan, W.F. Wang, T.R. and Hsu, C.M., "A Curvature-ovalization Measurement Apparatus for Circular Tubes under Cyclic Bending," *Exp. Mech.*, Vol. 38, No. 2, pp. 99-102 (1998).

Shamass, R., Alfano, G. and Guarracino, F., "On Elastoplastic Buckling Analysis of Cylinders under Nonproportional Loading by Differential Quadrature Method," *Int. J. Struct. Stab. Dyn.*, Vol. 17, No. 7,1750072 [40 pages] (2017).

Yazdani, H. and Nayebi, A., "Continuum Damage Mechanics Analysis of Thin-Walled Tube under Cyclic Bending and Internal Constant Pressure," *Int. J. Appl. Mech.*, Vol. 5, No. 4, 1350038 [20 pages] (2013).

Yuan, W. and Mirmiran, A., "Buckling Analysis of Concrete-Filled FRP Tubes," *Int. J. Struct. Stab. Dyn.*, Vol. 1, No. 3, pp. 367-383 (2001).

NOMENCLATURE

a_1 material parameter

a_2 material parameter

C material parameter

c_1 material parameter

c_2 material parameter

ℓ_{long} length of the long axis

ℓ_{short} length of the short axis

N_{b} number of cycles required to initiate buckling

M bending moment

α material parameter

$\Delta\ell$ change of the ℓ_{short}

κ curvature

κ_{o} dimensionless quantity of κ

不同長/短軸比橢圓管在循環彎曲負載下之響應與失效

余敏誠　潘文峰
國立成功大學工程科學系

摘 要

本研究探討了不同長/短軸長比（1.5、2.0、2.5和3.0）下，壁厚均為0.7 mm 的 SUS304不鏽鋼橢圓管在循環彎曲負載下的響應和失效。我們將循環彎曲負載施加於所有的橢圓管，直至挫曲失效出現。實驗中的彎矩-曲率關係呈現出循環硬化現象，並且會形成穩定的迴圈；增加長/短軸長比則稍微降低彎矩的峰值。關於實驗短軸變化和曲率之間的關係（其中短軸變化為短軸長度變化除以短軸的原始長度），我們觀察到，無論長/短軸長比為何，隨著循環次數的增加，這種關係呈現出對稱、棘齒和增加的趨勢。有趣的是，當長/短軸長比等於2.0、2.5和3.0時，上述關係甚至呈現出蝴蝶狀的趨勢。此外，較大的長/短軸長比對應出較大的短軸變化。從曲率-循環至挫曲圈數的關係中可以觀察到，當以雙對數座標繪製時，四種長/短軸長比分別對應到四條直線。最後，本研究提出了理論方程式來描述上述關係，並將理論分析與實驗數據進行比較，揭示了兩種方法之間的一致性。這證實該理論能夠合理地描述實驗結果。